

Supporting Information

Biocompatible, Flexible, and Oxygen-Permeable Silicone-Hydrogel Material for Stereolithographic Printing of Microfluidic Lab-on-a-Chip and Cell-Culture Devices

Sabine Zips[†], Lukas Hiendlmeier^{†‡}, Lennart Jakob Konstantin Weiß[†], Heike Url[†], Tetsuhiko F. Teshima^{†‡}, Richard Schmid[#], Markus Eblenkamp[#], Petra Mela[#], and Bernhard Wolfrum^{†‡§}*

[†] Neuroelectronics - Munich School of Bioengineering, Department of Electrical and Computer Engineering, Technical University of Munich, Boltzmannstr. 11, 85748 Garching, Germany

[‡] Medical & Health Informatics Laboratories, NTT Research Incorporated, East Palo Alto, California 94303, United States

[#] Chair of Medical Materials and Implants, Department of Mechanical Engineering, Technical University of Munich, Boltzmannstr. 15, 85748 Garching, Germany

[§] Institute of Biological Information Processing, Bioelectronics (IBI-3), Forschungszentrum Jülich, 52425 Jülich, Germany

S.Z. and L.H. contributed equally.

Corresponding Author

* Bernhard Wolfrum

E-Mail: bernhard.wolfrum@tum.de

Resin Formulation

The silicone-hydrogel resin was prepared from 53.13% (w/w) reactive diluent isobornyl acrylate (IBA; Sigma Aldrich, St. Louis, MO), 15% (w/w) silicone macromer DBE-U22 (Gelest, Morrisville, NC), 15% (w/w) silicone macromer UMS-182 (Gelest, Morrisville, NC), 15% (w/w) hydrogel hydroxyethyl methacrylate (HEMA; Sigma Aldrich, St. Louis, MO), 1% (w/w) cross-linker tetraethylene glycol diacrylate (TEGDA, Sigma Aldrich, St. Louis, MO), 0.5% (w/w) photoinitiator PI 2100 (Omnirad 2100, IGM Resins, Waalwijk, Netherlands; SpeedCure 2100, Lambson, Wetherby, United Kingdom), which is a blend from ethyl(2,4,6-trimethylbenzoyl)phenylphosphinat and bis(2,4,6-trimethylbenzoyl)phenylphosphine oxide, 0.35% (w/w) UV absorber 2-isopropylthioxanthone (ITX; Omnirad ITX, IGM Resins, Waalwijk, Netherlands; SpeedCure 2-ITX, Lambson, Wetherby, United Kingdom), and 0.02% (w/w) quencher 2,2,6,6-tetramethylpiperidine-1-oxyl (TEMPO; Sigma Aldrich, St. Louis, MO). The chemical structures of all components are shown in **Figure S1**.

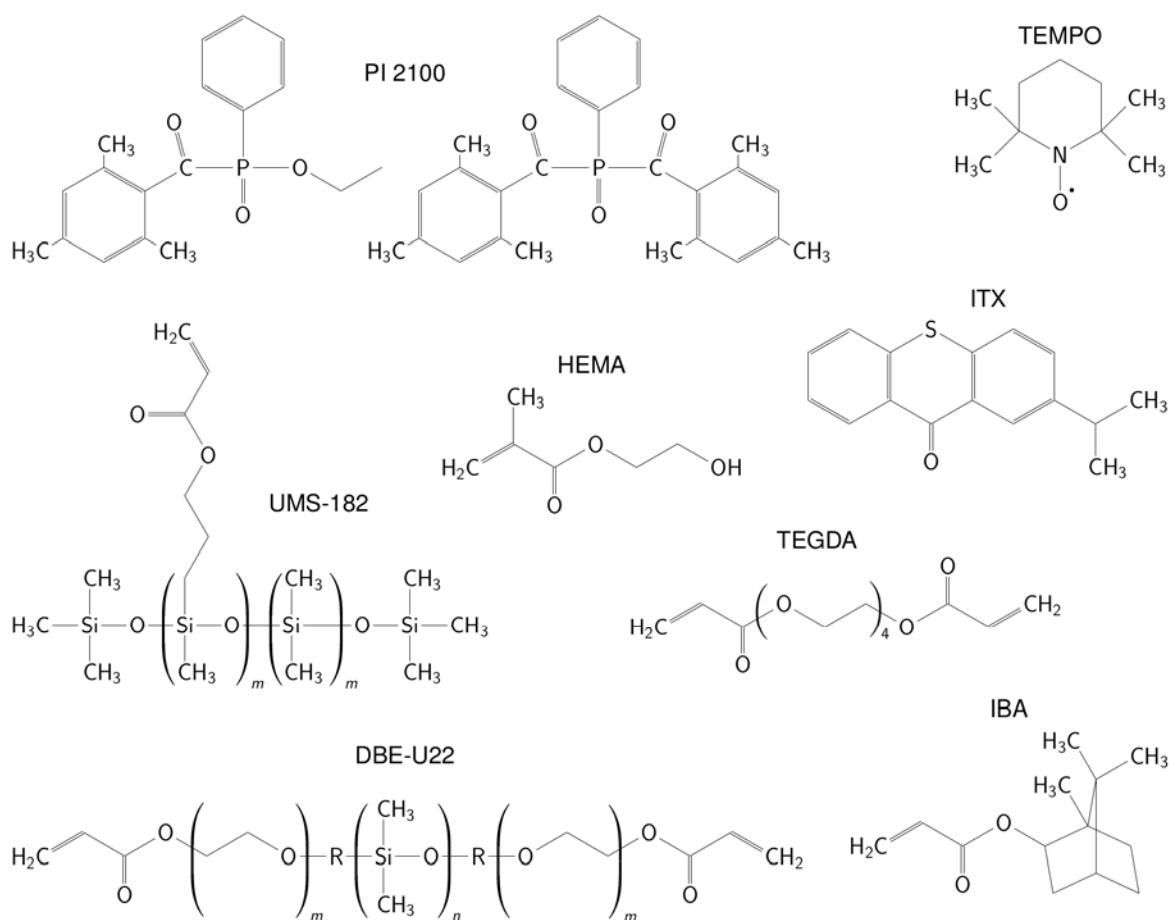


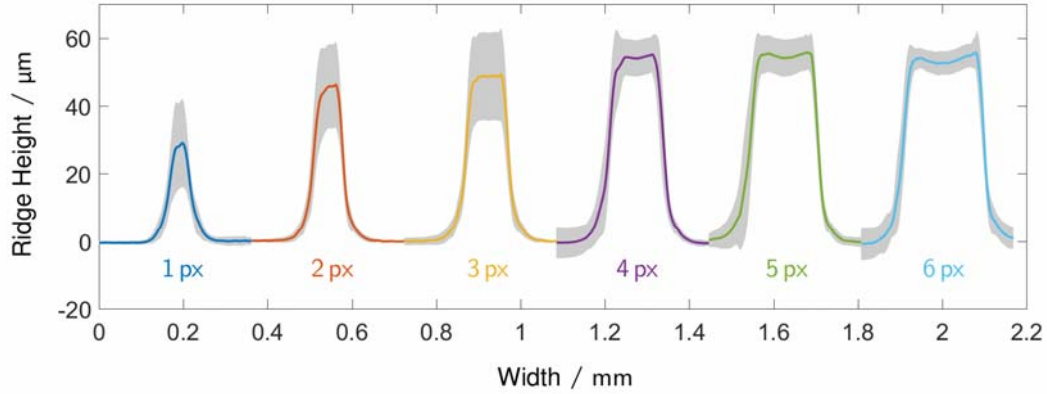
Figure S1. Chemical structures of the resin components.

Characterization of xy- and z-Resolution

For testing the lateral resolution, rectangular plates with positive or negative small features in the last, 50 μm high print layer (see CAD model in **Figure S2**) were fabricated with the MiiCraft 50X stereolithographic printer using an irradiance of 1 mW cm^{-2} and exposure time of 24 s. More specifically, the test layers contained wells, channels, bumps, and lines that were printed with integer pixel numbers ($1 \text{ px} = 30 \mu\text{m}$), i.e. the wells or bumps had sizes of $1\text{--}10 \text{ px}^2$ and the channels or ridges had widths of $1\text{--}6 \text{ px}$. The cross-sectional line plots of the surface scans of the test specimens are displayed in **Figure S3** and were used to measure the actual height and widths of the printed channel features. The data is shown in **Table S1**.

In addition, test structures with horizontal channels of varying widths and heights were printed to identify the minimum printable internal channel sizes. The prints were cut to cross sections and imaged with a contour analysis system to assess the print quality of the channels, i.e. channels with visible obstructions were regarded as non-functional. The complete evaluation is presented in **Table S2**. Similarly, channels printed as last-layer features and bonded onto silanized glass slides (3-(trimethoxysilyl)propyl methacrylate) were investigated and the results are given in **Table S3**.

a)



b)

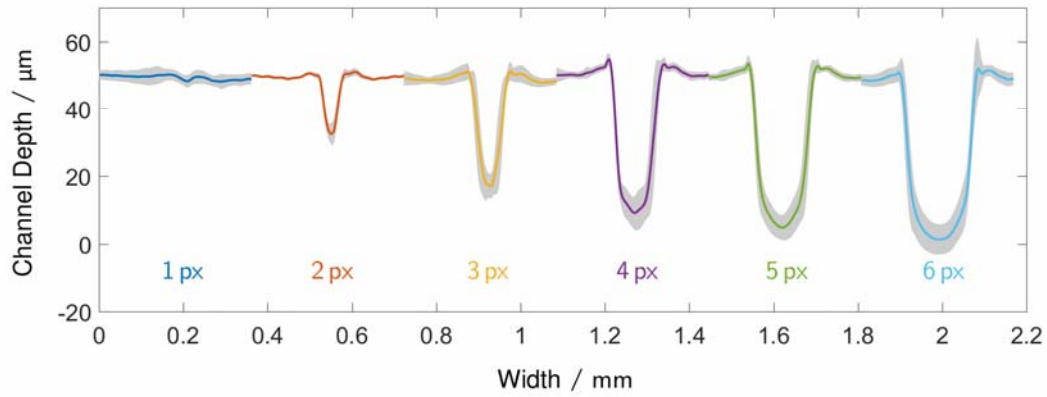


Figure S3. Average cross-sectional line plots of the printed **a)** lines and **b)** ridges taken from the surface scans ($n = 16$ test samples). The data is plotted with an arbitrary offset in x-direction for presentation reasons. The standard deviation is shown as shaded area. The colored numbers are the designed pixel widths of the test structures.

Table S1. Measured height and widths (FWHM) of the printed test structures, i.e. ridges and channels.

		Designed width in [px] and [μm]					
		1	2	3	4	5	6
		30 μm	60 μm	90 μm	120 μm	150 μm	180 μm
Ridges	Width [μm]	54 \pm 14	72 \pm 9	103 \pm 8	131 \pm 16	163 \pm 19	194 \pm 13
	Height [μm]	29 \pm 13	46 \pm 13	49 \pm 14	55 \pm 5	56 \pm 5	56 \pm 5
Channels	Width [μm]	n.a.	34 \pm 6	55 \pm 19	86 \pm 11	117 \pm 14	146 \pm 12
	Depth [μm]	n.a.	17 \pm 3	33 \pm 4	41 \pm 5	45 \pm 4	49 \pm 4

Table S2. Printing yield of inner channels. The average widths and heights of the measured channels (total of n = 10 prints) are given below the inset images.




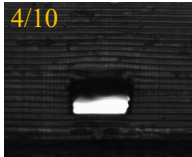
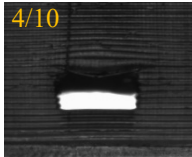
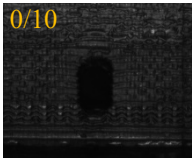
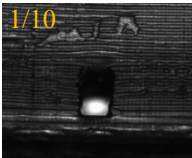
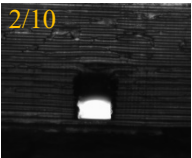
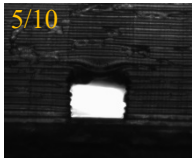

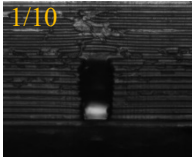
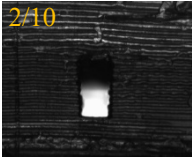
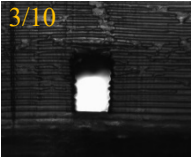
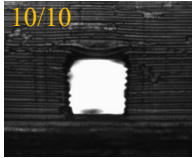
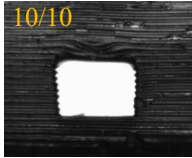
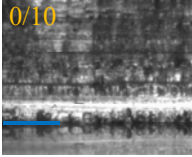
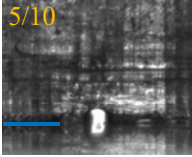
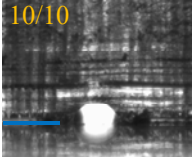
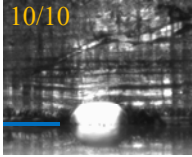
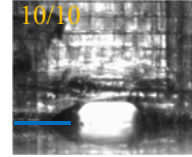
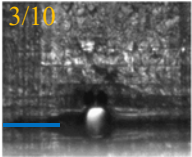
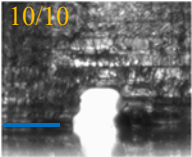
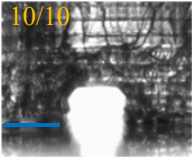
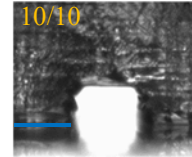
		Channel Width				
		8 px - 240 μm	9 px - 270 μm	10 px - 300 μm	15 px - 450 μm	20 px - 600 μm
Channel Height	300 μm					
	400 μm					
	500 μm					
					$\updownarrow 133 \pm 45 \text{ } \mu\text{m}$ $\leftrightarrow 414 \pm 14 \text{ } \mu\text{m}$	$\updownarrow 158 \pm 41 \text{ } \mu\text{m}$ $\leftrightarrow 585 \pm 15 \text{ } \mu\text{m}$
			$\updownarrow 111 \text{ } \mu\text{m}$ $\leftrightarrow 178 \text{ } \mu\text{m}$	$\updownarrow 138 \pm 28 \text{ } \mu\text{m}$ $\leftrightarrow 208 \pm 55 \text{ } \mu\text{m}$	$\updownarrow 161 \pm 68 \text{ } \mu\text{m}$ $\leftrightarrow 310 \pm 96 \text{ } \mu\text{m}$	$\updownarrow 232 \pm 54 \text{ } \mu\text{m}$ $\leftrightarrow 531 \pm 40 \text{ } \mu\text{m}$
		$\updownarrow 77 \text{ } \mu\text{m}$ $\leftrightarrow 165 \text{ } \mu\text{m}$	$\updownarrow 159 \pm 62 \text{ } \mu\text{m}$ $\leftrightarrow 206 \pm 12 \text{ } \mu\text{m}$	$\updownarrow 253 \pm 79 \text{ } \mu\text{m}$ $\leftrightarrow 252 \pm 19 \text{ } \mu\text{m}$	$\updownarrow 388 \pm 26 \text{ } \mu\text{m}$ $\leftrightarrow 417 \pm 25 \text{ } \mu\text{m}$	$\updownarrow 422 \pm 23 \text{ } \mu\text{m}$ $\leftrightarrow 599 \pm 25 \text{ } \mu\text{m}$

Table S3. Printing yield of bonded channels to silanized glass slides. The average widths and heights of the measured channels (total of $n = 10$ prints) are given below the inset images. The blue bars indicate the interface between the glass slides and the prints.

		Channel Width				
		1 px - 30 μm	2 px - 60 μm	3 px - 90 μm	4 px - 120 μm	5 px - 150 μm
Channel Height	50 μm					
	100 μm		$\updownarrow 40 \pm 8 \mu\text{m}$ $\leftrightarrow 41 \pm 15 \mu\text{m}$	$\updownarrow 50 \pm 8 \mu\text{m}$ $\leftrightarrow 89 \pm 17 \mu\text{m}$	$\updownarrow 52 \pm 9 \mu\text{m}$ $\leftrightarrow 120 \pm 17 \mu\text{m}$	$\updownarrow 48 \pm 9 \mu\text{m}$ $\leftrightarrow 150 \pm 12 \mu\text{m}$
	50 μm					
	100 μm		$\updownarrow 45 \pm 8 \mu\text{m}$ $\leftrightarrow 45 \pm 17 \mu\text{m}$	$\updownarrow 79 \pm 24 \mu\text{m}$ $\leftrightarrow 81 \pm 18 \mu\text{m}$	$\updownarrow 100 \pm 7 \mu\text{m}$ $\leftrightarrow 129 \pm 19 \mu\text{m}$	$\updownarrow 95 \pm 8 \mu\text{m}$ $\leftrightarrow 149 \pm 19 \mu\text{m}$

Flexibility and Tensile Strength

Measurements for the tensile strength were conducted following ISO 527-1:2012 (the test rods were down-scaled according to ISO 20753:2018 to the build size of the MiiCraft 50X printer). Dry and wet silicone-hydrogel material was compared to the commercial resin MedicalPrint Clear and PEGDA-250-ITX, a resin based on the hydrogel poly(ethylene glycol) diacrylate (PEGDA, M_n 250). The printed test specimens had an initial tapered gauge length of 20 mm with a cross sectional area of $3.33 \times 2 \text{ mm}^2$ (width \times thickness, see **Figure S4a**). The printed and post-processed specimens were clamped into an automatic tensile tester and stretched with constant 2 mm min^{-1} . The engineering stress $\sigma = F / A$ (in units of N m^{-2} or Pa, F is the applied force, A is the nominal cross section of the specimen) was recorded against the engineering strain $\varepsilon = \Delta L / L_0$ (elongation of the gauge section $\Delta L = L - L_0$ with respect to the initial gauge length L_0) in a stress-strain curve. The slope of the data curves in the linear elasticity regime – here case 0–5% elongation was taken as the Young's Modulus of the material (see **Equation 2**),

$$E = \frac{\Delta\sigma}{\Delta\varepsilon}.$$

The obtained stress-strain curves for dry and wet silicone-hydrogel material, MedicalPrint Clear, and PEGDA-250-ITX are shown in **Figure S4c**. The mechanical properties of all measured materials are summarized in **Table S3**.

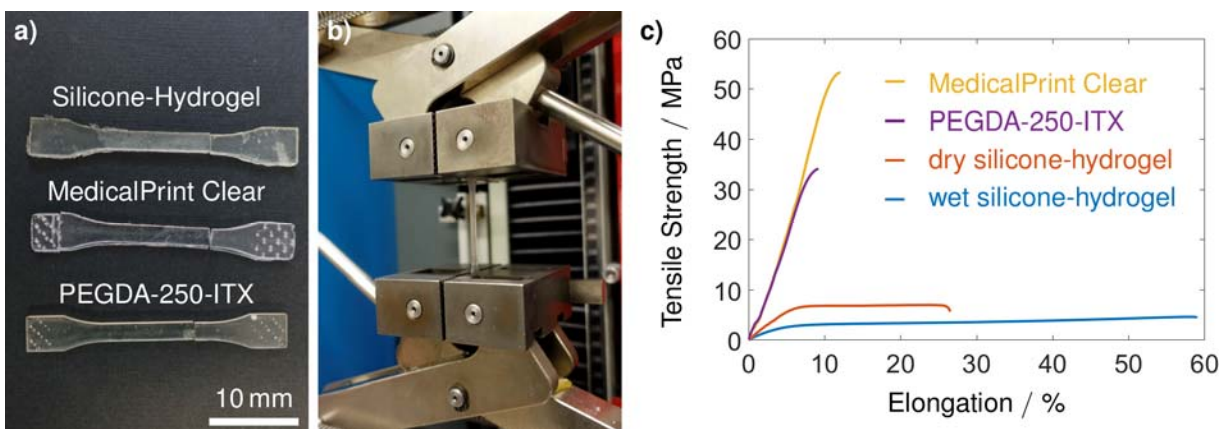


Figure S4. a) Example test specimens from silicone-hydrogel material, MedicalPrint Clear, and PEGDA-250-ITX, which were b) stretched with constant 2 mm min^{-1} until breakage in a tensile tester (Zwick Z2.5, Zwick-Roell, Ulm, Germany). c) Stress-strain curves for dry and wet silicone-hydrogel, MedicalPrint Clear, and PEGDA-250-ITX.

Table S4. Mechanical Properties of dry and wet silicone-hydrogel polymer, MedicalPrint Clear, and PEGDA-250-ITX ($n = 9$ each, average \pm standard deviation).

Material	Tensile Strength [MPa]	Young's Modulus [MPa]	Elongation at Break [%]
Dry Silicone-Hydrogel Material	7 ± 1	138 ± 17	21 ± 13
Wet Silicone-Hydrogel Material	5 ± 1	78 ± 18	51 ± 11
MedicalPrint Clear	52 ± 4	415 ± 71	12 ± 1
PEGDA-250-ITX	30 ± 3	399 ± 40	8 ± 1

Bonding onto Surface-Treated Glass Substrates

Glass slides and cut-outs of polyethylene naphthalate (PEN) foil (Teonex Q65HA, DuPont Teijin Films, Hopewell, VA) were silanized with 3-(trimethoxysilyl)propyl methacrylate. The cleaned, but not further post-processed prints can simply be pressed onto the treated glass and PEN substrates. The post-curing of the assembled devices with UV light in inert gas atmosphere then bonds the two parts. The adhesion strength was measured using printed cylinders that were bonded onto treated substrates and pulled with a tensile tester (see **Figure S5**). The dry and wet specimens on glass (water-immersed for at least 24 h before measurements, $n = 9$ samples each) sustained the minimum engineering stresses of 1.6 MPa and 1.7 MPa, respectively, above which either the printed test bodies or the glass slides broke, while the interface of print/glass remained intact. The samples on PEN foil sustained stresses of 0.4 ± 0.2 MPa ($n = 5$, silicone-hydrogel polymer in dry state, measured minimum stress of 0.2 MPa) before the foil ripped and the test bodies were partly peeled off.

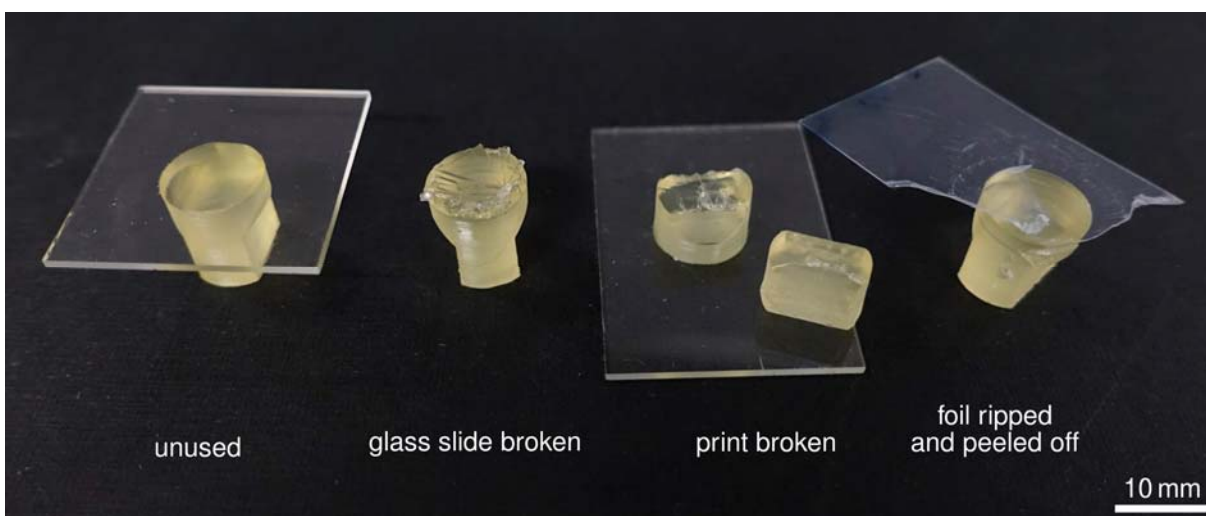


Figure S5. Printed test bodies in silicone-hydrogel material bonded onto silanized glass slides and PEN foils. The test specimens were pulled with a tensile tester, which resulted in the breakage of the glass slide, ripping of the printed test body at the clamping section, or ripping of the PEN foil.

Biocompatibility with Respect to Different Sterilization Methods

Printed test stripes ($25 \times 5 \times 2 \text{ mm}^3$) of silicone-hydrogel material were either sterilized by dipping in 2-propanol and drying, exposure to UV light for over 20 min (UV chamber from NK-Optik, Baierbrunn, Germany), or exposure to saturated hot steam (1 h at 1 bar and 120 °C, Autoklav 23, Melag, Berlin, Germany). The samples were first pre-extracted in cell-culture grade sterile water for 18–24 h and then extracted for 7 days in medium at 37 °C in 5% CO₂ atmosphere in a humidified incubator. The WST-8 cell viability assay was performed with respect to cardiomyocyte-like HL-1 cells and HT1080 fibroblasts for two rounds of cell cultures. The cytotoxicity results for the different sterilization methods are shown in **Figure S6**. The material does not cause an inhibition of the cell viability above 30% and is thus, biocompatible for all of the three sterilization methods with respect to the tested cell types.

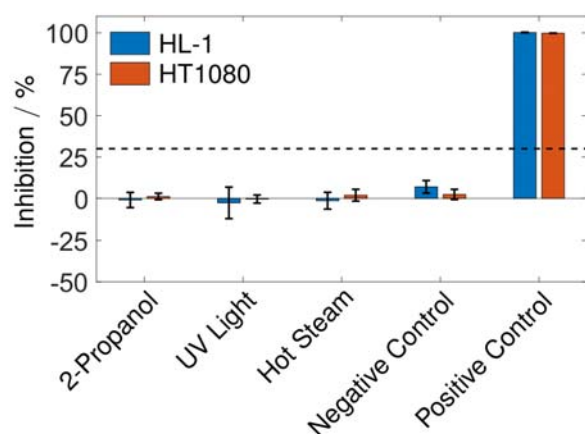


Figure S6. WST-8 cytotoxicity test results for silicone-hydrogel material and different sterilization methods, i.e. 2-propanol, UV light, or saturated hot steam.

Growth Test of HT1080 Fibroblasts on Surface-Coated Silicone-Hydrogel Material

Culture dishes were SLA printed in the silicone-hydrogel material (see CAD model in **Figure S7**). For coating with fibronectin and gelatin, the printed dishes were post-cured with 2000 flashes under nitrogen influx (Otoflash G171 UV curing chamber, NK-Optik, Baierbrunn, Germany), O₂-plasma treated for increased wettability (0.8 mbar at 80 W for 5 min; Diener Femto, Diener electronic, Ebhausen, Germany), sterilized by dipping in 2-propanol and drying, and incubated in a solution of fibronectin/gelatin (5 $\mu\text{g ml}^{-1}$ /0.2 mg ml^{-1}) and water for approximately 24 h at 37 °C in 5% CO₂ in a humidified incubator for extraction and coating. For grafting of gelatin methacryloyl (GelMA, gel strength 300 g bloom, degree of substitution 60%, Sigma Aldrich, St. Louis, MO) onto silicone-hydrogel culture dishes, a volume of 50 μl of GelMA solution (10% w/w in water) was pipetted into the cleaned, but not further post-processed wells and then polymerized with 1000 flashes under nitrogen influx. Unbound residues of GelMA were rinsed off with water. The samples were then blow-dried and post-cured with additional 2000 flashes. Next, the dishes were sterilized by dipping in 2-propanol and drying, and extracted in water for approximately 24 h at 37 °C in 5% CO₂ in a humidified incubator. Before cell seeding, the samples (n = 9 wells for each coating type) were briefly rinsed with medium and fibroblasts HT1080 were then seeded onto the dishes in a density of 30k per well. The medium was exchanged on DIV1 and the cell layers were imaged via life-dead staining on DIV2. For staining, the cells were incubated in a solution of Calcein-AM (4 μM , ThermoFisher Scientific, Waltham, MA) and ethidium homodimer (2 μM , ThermoFisher Scientific, Waltham, MA) in serum-free medium for 15 min at 37 °C. The staining solution was aspirated, the cell layers were rinsed, and fresh medium was added. After an additional incubation time of 10 min at 37 °C, the samples were imaged with a fluorescence microscope (Leica DM 2700 M, Leica, Wetzlar, Germany). The HT1080 cell layers showed a healthy cell morphology and strong green fluorescence (see **Figure S8**) in both fibronectin/gelatin and GelMA coated silicone-hydrogel culture dishes. Untreated samples (printed, post-cured with 2000 flashes, sterilized by dipping in 2-propanol and drying, extracted in water for 24 h at 37 °C in 5% CO₂) did not support cell growth.

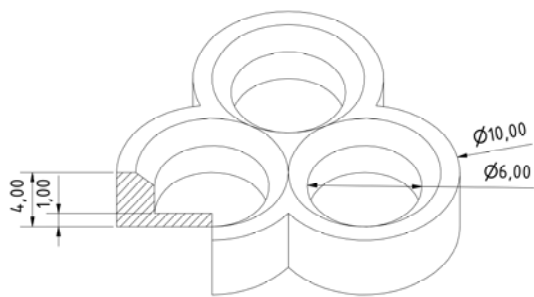


Figure S7. CAD model of the printed cell-culture dishes.

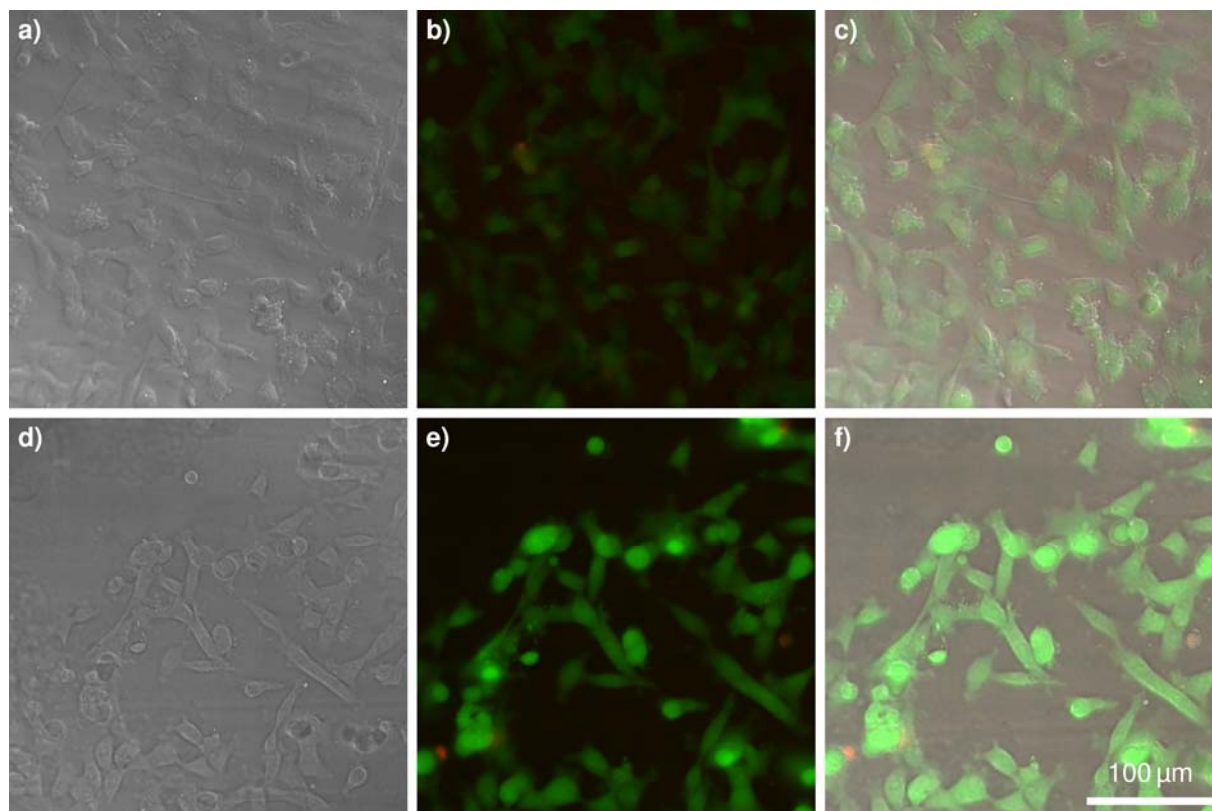


Figure S8. Life-dead staining of HT1080 fibroblast cell layers growing on **a)-c)** fibronectin-gelatin coated silicone-hydrogel culture dishes and **d)-f)** GelMA grafted onto silicone-hydrogel culture dishes.

Non-Specific Adsorption of Small Hydrophobic Molecules

Printed silicone-hydrogel test stripes ($25 \times 5 \times 2 \text{ mm}^3$, $n = 3$ test stripes for each coating type) were partly surface functionalized with hydrophilic PEG by post-curing in either a PEGMA solution (1:1 v/v in water) or PEGDA-250 with 1000 flashes under nitrogen influx (Otoflash G171 UV curing chamber, NK-Optik, Baierbrunn, Germany). The residues of uncured monomers were rinsed off with water and the samples were then fully cured with 2000 flashes under nitrogen influx. For testing the non-specific adsorption of a small hydrophobic molecule, a solution of Nile red (1 mM in 1:1 w/w water/DMSO) was drop-cast onto the test stripes across the interface of the surface-coated and untreated areas. The solution was allowed to incubate for 30 s, washed off with water, and the samples were imaged with a fluorescence microscope (Leica DM 2700 M, Leica, Wetzlar, Germany). The PEGMA-treated silicone-hydrogel surfaces showed an increased non-specific adsorption of Nile red in comparison to the untreated silicone-hydrogel surfaces, the PEGDA-250 surfaces showed a significantly decreased adsorption of Nile red (see **Figure S9**). This points towards potential routes for the modulation of the adsorptive properties of the silicone hydrogel material.

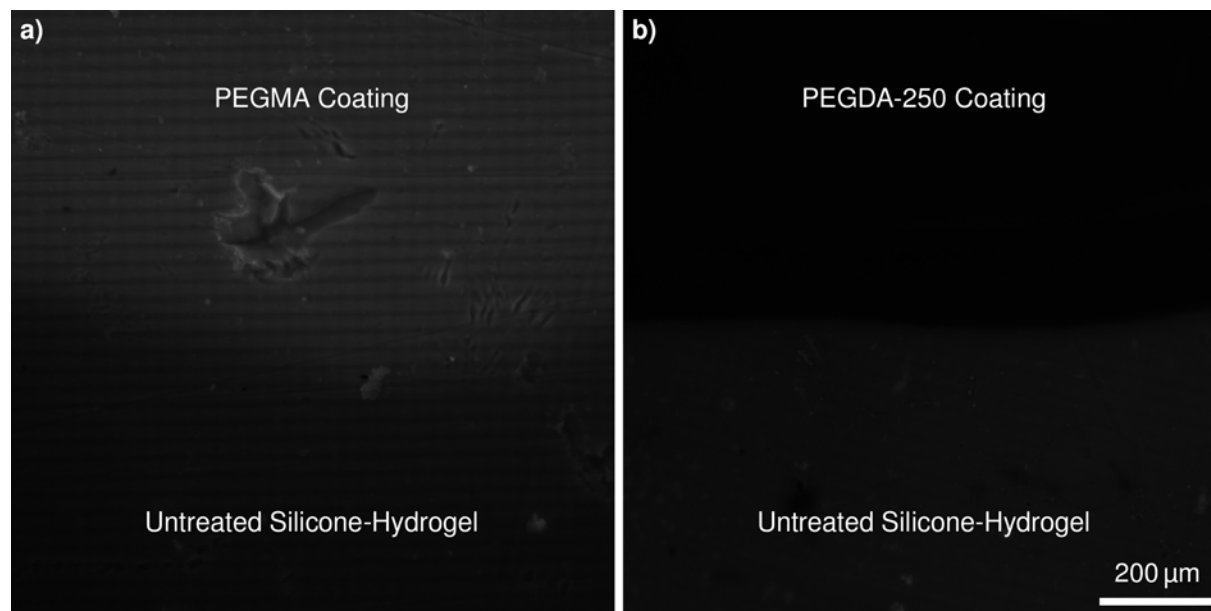


Figure S9. Non-specific adsorption of the small hydrophobic molecule Nile red on **a)** PEGMA-functionalized silicone-hydrogel surfaces, or **b)** PEGDA-250 treated silicone-hydrogel surfaces.

Oxygen Permeability

The oxygen permeability of the silicone-hydrogel material, PDMS, the commercial MedicalPrint Clear, and PEGDA-250-ITX was measured using a sensing device from the oxygen-sensitive fluorophore platinum octaethylporphyrin (PtOEP). The CAD model of the printed test system is shown in **Figure S10**. The system features two chambers, one comprising a polystyrene sensing membrane with embedded PtOEP. The second chamber is separated from the first by a 170 μm thick layer of adhesive tape and a 110 ± 10 μm thick membrane from dry or wet silicone-hydrogel material, PDMS, MedicalPrint Clear, or PEGDA-250-ITX. The second chamber was connected to nitrogen and air supply. At the start of the measurement, nitrogen was flushed through the second chamber for 30 min to draw out the oxygen present in the fixed volume between the membrane and the PtOEP sensing area. Then, the second chamber was brought back to atmospheric conditions and the fluorescence quenching was observed while oxygen was allowed to diffuse back into the first chamber across the membrane. The gas permeabilities were calculated with COMSOL using a 1D model of time-dependent transport of diluted species. An overview of all the equations, parameters, boundary and starting conditions is given in **Table S5**. The oxygen transport from the second chamber through the membrane and first sensing chamber to the sensing area was modelled using Fick's second law of diffusion in **Equation 4**, Henry's law in **Equation 5**, and the Stern-Volmer relation in **Equation 6**, where c_m , c_1 , c_2 , c_s are the oxygen concentrations in the membrane, the (first) sensing chamber, the second gas chamber, or at the sensor, respectively, x is the distance from the second chamber to the sensor area through the membrane and the first chamber, D_m and D_1 (D_1 assumed to be equal to the diffusion constant of oxygen in air D_{air}) are the diffusion coefficients of oxygen in the membrane or the sensing chamber, respectively. S_m and S_1 are the Henry's constant as a measure of oxygen solubility in the membrane

and the sensing chamber, respectively, and p_1 and p_2 are the partial pressures of oxygen at room temperature in the first and the second chamber, respectively. I_0 is the fluorescence intensity for 0% oxygen concentration obtained by the calibration and k is the calibrated Stern-Volmer constant for PtOEP in polystyrene, which was obtained from cycling between 0% and 21% oxygen concentrations before insertion of the material membranes and applying a linear fit to the relation $(I_0/I) - 1$ vs c_s .

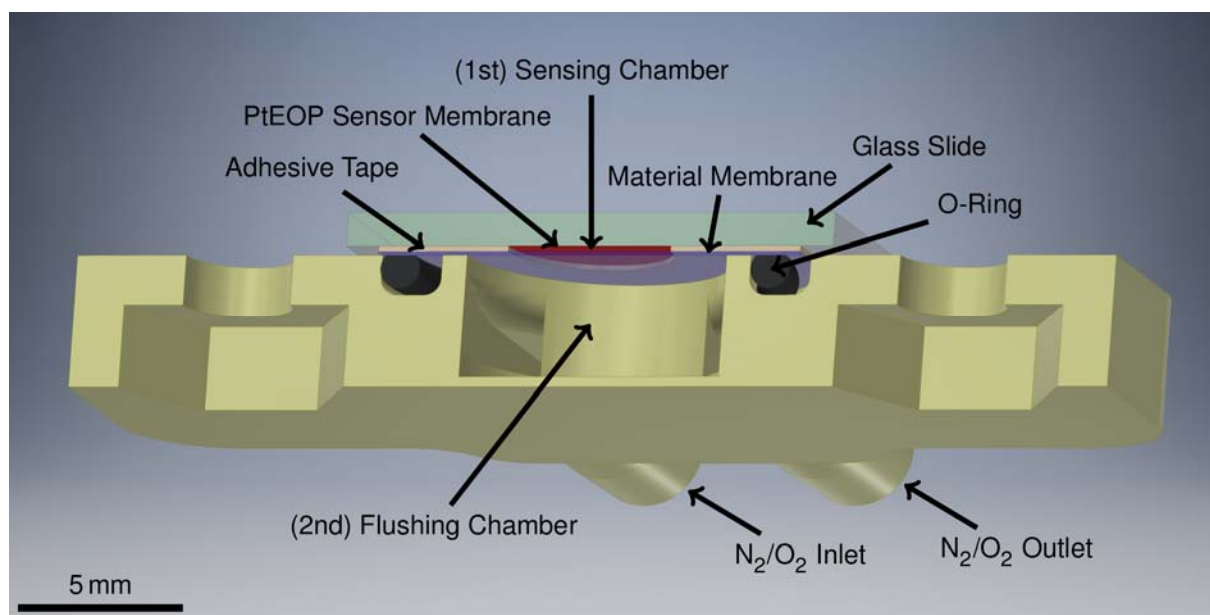


Figure S10. Schematic of the test system for measuring the oxygen permeability of the 3D-printing materials.

Table S5. COMSOL model for time-dependent 1D transport of diluted species.

	2 nd Chamber	Membrane	1 st Chamber	Sensor
	(air supply N ₂ / O ₂)	(material)	(sensing chamber)	(PtOEP membrane)
x-Dimension	Interface	110 μm	170 μm	Interface
	$x = 0$		$x = 110 \mu\text{m}$	$x = 280 \mu\text{m}$
Governing Equations, Boundary and Starting Conditions	Uptake of O ₂ into Membrane Henry's Law Fixed Concentration Condition $c_m(x = 0, t) = p_2 S_m$ $= \text{const}$ with $p_2 = pO_2 = 21 \text{ kPa}$	Diffusion Transport Fick's 2 nd Law $\frac{\partial c_m(x, t)}{\partial t} = D_m \frac{\partial^2 c_m(x, t)}{\partial x^2}$ $c_m(x, t = 0) = \frac{S_m}{S_1} c_1(x, t = 0)$ $= \frac{S_m}{S_1} c_{s,0}$	Release of O ₂ from Membrane Henry's Law Partition Condition $p_1 = \frac{c_m(x = 110 \mu\text{m}, t)}{S_m}$ ideal gas at room temperature $c_1(x, t = 0) = \frac{1}{k} \left(\frac{I_0}{I(c_{s,0})} - 1 \right) = c_{s,0}$	Henry's Law $c_s = p_1 S_1$ Fluorescence Quenching Stern-Volmer Equation $\frac{I_0}{I(c_s)} = 1 + kc_s$ $c_s(x = 280 \mu\text{m}, t = 0) = c_{s,0}$ $I(c_s = 0 \%) = I_0$ No-Flux Boundary Condition

Printed Microfluidic Proof-of-Concept Device

A microfluidic structure with integrated valves and mixers (see CAD model in **Figure S11**) was printed in the silicone-hydrogel resin, cleaned, dried, pressed top-down onto a silanized glass slide, and post-cured (2000 flashes under nitrogen influx, Otofash G171 UV curing chamber, NK-Optik, Baierbrunn, Germany).

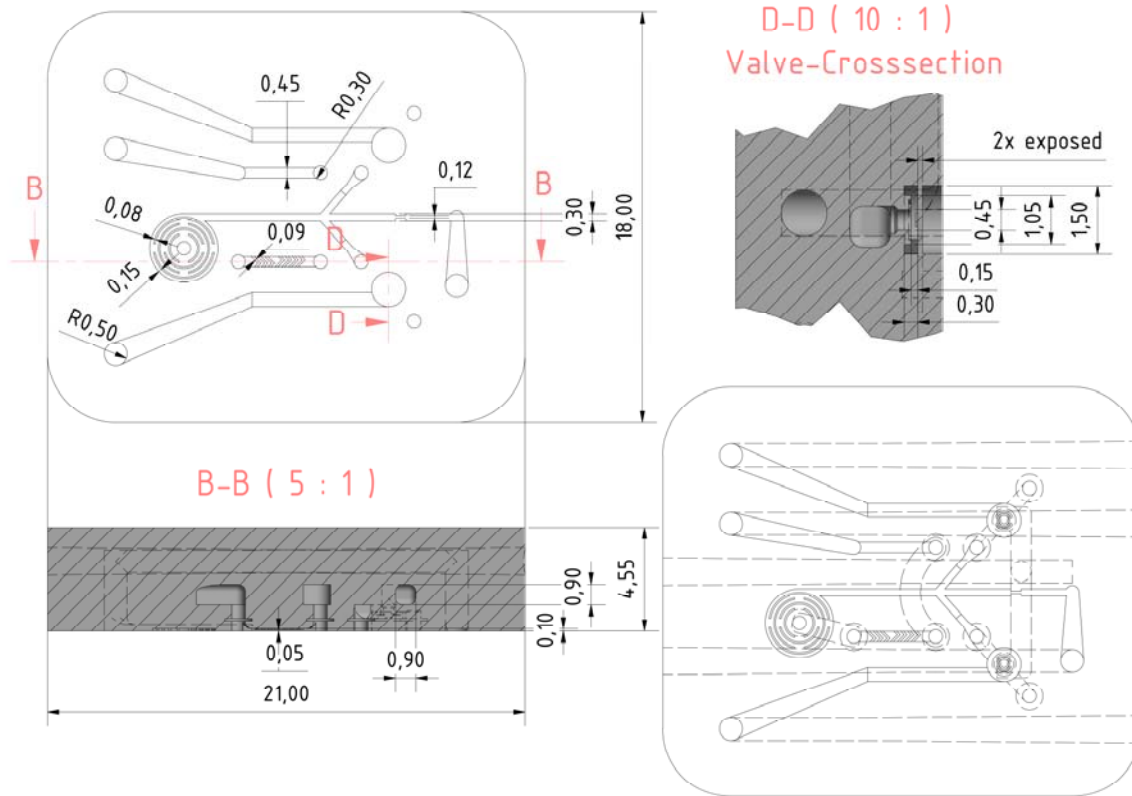


Figure S11. CAD model of the microfluidic proof-of-concept device.